Radio-fluorogenic, solid-state polymer dosimeter for recording depth-dose profiles related to radiation processing of surfaces

Skowyra, M. M.; Lindvold, L.R.

Published in:
Radiation Measurements

Link to article, DOI:
10.1016/j.radmeas.2020.106383

Publication date:
2020

Document Version
Peer reviewed version

Journal Pre-proof

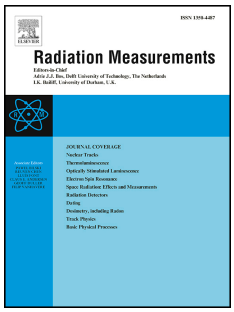

Radio-fluorogenic, solid-state polymer dosimeter for recording depth-dose profiles related to radiation processing of surfaces

M.M. Skowyra, L.R. Lindvold

PII: S1350-4487(20)30162-1

DOI: https://doi.org/10.1016/j.radmeas.2020.106383

Reference: RM 106383

To appear in: *Radiation Measurements*

Received Date: 30 October 2019

Revised Date: 25 March 2020

Accepted Date: 12 May 2020

Please cite this article as: Skowyra, M.M., Lindvold, L.R., Radio-fluorogenic, solid-state polymer dosimeter for recording depth-dose profiles related to radiation processing of surfaces, *Radiation Measurements* (2020), doi: https://doi.org/10.1016/j.radmeas.2020.106383.

P1-029

Radio-fluorogenic, solid-state polymer dosimeter for recording depth-dose profiles related to radiation processing of surfaces

Skowyra, M.M.[a], Lindvold L.R.[b]

[a,b] *DTU Health Tech, Technical University of Denmark, Frederiksborgvej 399, Building 201, 4000 Roskilde, Denmark*

[a] *magsk@dtu.dk,* [b] *lali@dtu.dk*

HIGHLIGHTS

- Fluorescence response of the solid-state dosimeter can be measured by using epi-fluorescence microscopy
- The fluorescence signal serves as a tool to obtain depth-dose distributions of low-energy electron beams
- Measured depth-dose profiles may be used as a dose verification in radiation processing of surfaces

ABSTRACT

The use of ionizing radiation in industrial radiation-processing applications is well-known and low-energy electron beam accelerators are gaining in importance, as they offer several advantages over isotope radiation sources. In this study, a solid-state, polymer material, which responds to high radiation doses by the change in fluorescence intensity, is presented. The ease of photopolymerization process allows curing of the dosimeter in any shape. The signal is measured with an epi-fluorescence microscope and the image processing of the obtained scans can be used to record relative dose-depth distributions of low-energy electron radiations.

KEYWORDS

radiation processing, dosimetry, fluorescence, solid-state polymer dosimeter, pararosaniline leuco dye

1. Introduction

Radiation processing is accepted to a large degree in three main areas of the industry: 1) sterilization of single-use medical devices, 2) food irradiation and 3) polymer properties modification (ICRU, 2008; IAEA, 2004). Its main advantage is achieving reproducible effects on a product, for the known absorbed radiation dose. In the last decades, electron beam accelerators turned out to be more and more attractive in terms of cost, reliability and with no radioactive waste to dispose of (Guozhong Wu, 2019). Compared to other none-radiation based industrial methods, e-beam processing does not leave any residuals on products, does not produce toxic volatiles and leaves the irradiated products ready to use immediately after processing (IAEA, 2008). Low-energy e-beam equipment became the fastest growing area for surface curing of inks and coatings, as well as for surface sterilization of a pharmaceutical component (Berejka A.J., 2014). The very low penetration depth of low-energy electrons could be also utilized for the decontamination of packaging materials and sterilization of grains by killing the surface bacteria (Guozhong Wu, 2019).

To achieve the necessary effect on the irradiated product, the radiation dose applied has to be controlled. Several routine dosimetry systems are available to fulfil the dosimetry requirements in radiation processing e.g. alanine-EPR, calorimeters, PMMA dosimeters, Fricke gels or radiochromic dye films (ICRU, 2008). The selection of a suitable dosimeter depends on a dose range and on various characteristics of the systems. However, the readout of the absorbed radiation dose information of those dosimeters is not performed in three dimensions and the dose gradients over the thickness of the dosimeter have to be corrected by introducing a concept of the dose in the first micrometer

- D_μ (Helt-Hansen J., 2010). Depth-dose distributions are measured as a part of this approach, using thin film dosimeters that are approximately 20 μm in thickness, so that the measurement closest to the surface is obtained by extrapolation of the depth dose curve. Hence, a new approach that would enable direct measurements of dose distributions in the first microns of a material is essential. The verification of irradiation processes with products of different shapes could be introduced by using this approach as well.

In this paper, we present a potential dosimetry system for verification of surface dose and depth-dose distributions of irradiated material using low-energy electron beams of energies 150-200 keV. We propose a 3D, polymer and solid-state dosimeter that may serve as a tool for the characterization of radiation facilities and process validation. The system is based on a photo□curable monomer blend doped with a radiochromic and radio-fluorogenic dye (McLaughlin W.L., 1977; Bernal-Zamorano M.R., 2017). Its main mechanism is based on the conversion of non-fluorescent leuco dye into the fluorescent form while irradiated by placing it in a rigid polymer matrix. Epi-fluorescence microscopy and image processing of the obtained microscope scans enable recording relative depth-dose distributions.

2. Materials and Methods

2.1. Fabrication process

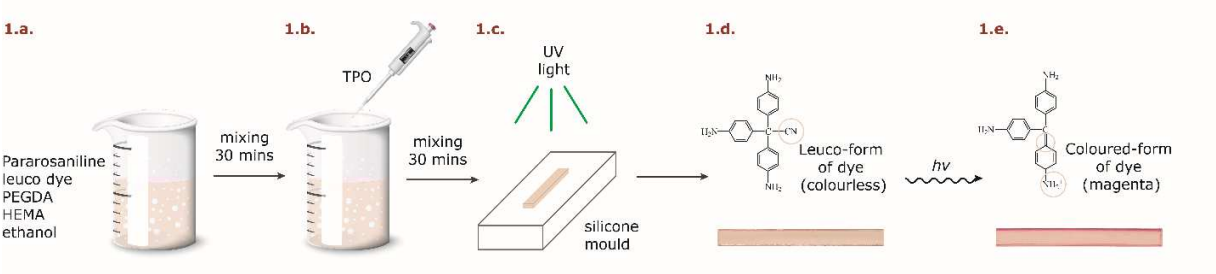

Fig 1. Schematic illustration of the preparation process of a dosimeter, explained in Materials and Methods section.

Pararosaniline leuco dye plays a key role in a dosimeter, causing its change in colour from a colourless leuco dye to a magenta dye, by the effect of ionizing radiation (ICRU, 2008). **Fig 1.** shows a simplified scheme of a manufacturing process. The dye (5.56 mM, *NCK A/S*) was dissolved in PEGDA-575 (poly(ethylene glycol) diacrylate, 1.68 M, *Sigma Aldrich CAS: 6570-48-9*), which serves as a matrix and determines the main physical properties of the dosimeter, HEMA (2-Hydroxyethyl methacrylate, 0.74 M, *Sigma Aldrich CAS: 868-77-9*) and ethanol (0.77 M, *VWR Chemicals CAS:64-17-5*) (**Fig 1.a.**). They were mixed together for 30 minutes using vortex mixer (*Heidolph Instruments GmbH & CO. KG*). After that, a photoinitiator - TPO (diphenyl (2,4,6-trimethylbenzoyl) phosphine oxide, 1.29 mM, *Sigma Aldrich CAS: 75980-60-8*) was added (**Fig 1.b.**) and it was mixed for another half an hour. The properties of the material enable its curing through a photopolymerization process (Bernal-Zamorano M.R., 2017).

The photopolymer mixture was moulded from a silicone elastomer mould and cured using a LED lamp, as presented in **Fig 1.c**. The samples were then irradiated with a low-energy electron beam. To determine depth-dose distributions, the epi-fluorescence microscope and image processing of the obtained images were applied.

The mould was formed by using SYLGARD^{TM} 184 Silicone Elastomer Kit (*Dow Europe, GmbH*). 50 ml of silicone elastomer base and 5 ml of silicone elastomer curing agent were mixed in a paper cup. In order to remove air bubbles, the mixture was placed inside a glass vacuum desiccator that was connected to a diaphragm vacuum pump (*Divac 1.2L, Leybold GmbH*). A cuboid metal mould, with dimensions 3x30x3 mm, was placed in the middle of a plastic Petri dish and the silicone mixture was poured onto that. Then, it was put into an oven, which was set at 60 □C, and left for 48 hours for curing. The final form of the mould was cut by using a scalpel.

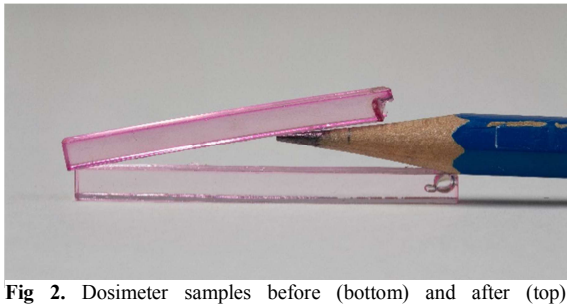

Fig 2. Dosimeter samples before (bottom) and after (top) irradiation (200 keV electron beam)

1 ml of photopolymer mixture (**Fig 1.c.**) was drawn up from the glass

vial and transferred to silicone mould. The mould was pressed to a glass microscope slide, in order to avoid leaking of the solution. After pouring the mixture, a rectangular plastic foil was placed on the top surface, to limit the amount of oxygen during the polymerization. The photo-curing was performed by using a 385 nm LED lamp, illuminating the sample from the top. The process took in total 3 minutes: 2 minutes exposure to light at a distance 10 cm, and 1 minute at 0.5 cm. A cured sample, like a one presented in the bottom part of **Fig. 2,** was removed from the mould and was ready for irradiation.

2.2. Irradiation

Irradiations were carried out using low energy electron beams of energies 150 keV and 200 keV, coming from an electron beam accelerator (*EBLab-200, COMET AG*). For both energies, three different surface doses were applied: 20 kGy, 30 kGy and 40 kGy, creating beam currents of 2.35, 3.52 and 4.70 mA for 150 keV and 3.10, 4.65 and 6.20 mA for 200 keV, respectively. The air gap was set to 10 mm with 15 m/min speed. As shown in **Fig 1.d.** and **Fig 1.e**, the irradiation caused a change in the chemical structure of the leuco dye, creating the magenta-coloured profile, also presented in **Fig 2.** (top).

2.3. Readout process

The fluorescence signal was measured by using a modified version of an epi-fluorescence microscope (*Axioskop 2FS MOT, Carl Zeiss Microscopy GmbH*). Each sample was placed in a glass container filled with an index matching fluid (*DC550, CAS: 63148-52-7*), to prevent the excitation light from being reflected, refracted and scattered at the surface of the sample. Filter set 20 (*Carl Zeiss Microscopy, GmbH*), which contains excitation (*BP 546/12*) and emission (*BP 575-640*) filters, was mounted, to achieve optimal transmission window in accordance with absorption and fluorescence spectra reported by Bernal-Zamorano M.R., 2017. The excitation wavelength peaks at 546 nm with 12 nm bandwidth and the emission has a bandwidth from 575 to 640 nm. HAL100 halogen illuminator (*Carl Zeiss Microscopy, GmbH*) was installed as an incident light illuminator. The images were captured using Point Grey camera (*FL3-U3-32S2C-CS, FLIR® Systems*), operated by FlyCapture® software. The images were processed using the Fiji package, based on ImageJ software. The autofluorescence signal coming from samples remained on a quite meaningful level, hence, the MosaicSuite plugin (©MOSAIC Group, MPI-CBG, Dresden) was used to remove the background noise. The autofluorescence is caused by several factors. First, the polymer matrix itself contributes to the effect, as some of the acrylate monomers constituting the solid-state dosimeter are autofluorescent (Chiu Y., 2012) even when excited with visible light at 520 nm due to by-products of the photoinitiator. Additionally, any leuco dye transformed to a free dye by ambient UV light or even the photocuring process will generate a bias autofluorescence signal. From dosimeter point of view, it is a disadvantage, as it lowers the signal-to-noise ratio and reduces the dynamic dose range.

Fig.4. Simplified scheme of the readout process

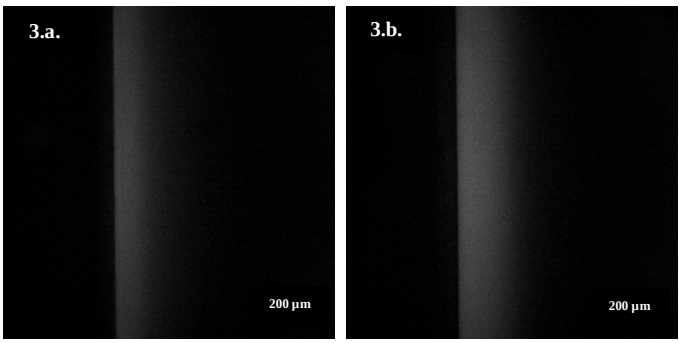

Fig 3. Fluorescence microscope scan of a dosimeter irradiated with **3.a.** 150 keV, **3.b.** 200 keV electron bean

3. Results and Discussion

The profiles of dosimeters irradiated with 150 keV and 200 keV electrons were captured by the camera from the top, as shown in **Fig 3.a.** and **Fig 3.b**, respectively. The dashed line indicates the surface of a sample; while black and white denote the minimum (0) and maximum (256) intensity of an 8-bit grayscale image, respectively. **Fig 4.** presents a scheme of the readout process. The fluorescence intensity profiles were calculated as the mean pixel value of each column of the image. The translation from pixel

P1-029

dimensions to SI units was carried out using the 1951 USAF resolution test chart (*ThorLabs, Inc.*) and the values were normalized to their maximum brightness. The autofluorescence background noise was reduced digitally, by using background subtractor from the MosaicSuite plugin. The relative dose-depth profiles were obtained, as presented in **Fig 5.a.** and **Fig 5.b.** The remaining tail signal, coming mainly from the signal outside of the focused area and instrument setup e.g. illumination intensity profile of the lamp, filters or camera noise, remained on a quite significant level and should be further reduced in order to finally relate the obtained scans to the absolute absorbed radiation dose. Nonetheless, one may observe that irradiation with the higher electron energy causes deeper penetration depth into the material and less steep dose gradient as for the lower energy. A small build-up region is also more noticeable for 200 keV (up to ~100µm), where the delivered dose level is fairly uniform. The shapes of the curves for different doses (meaning different electron beam currents) are similar, as expected. To estimate roughly the measured electron ranges, the CSDA ranges (Berger M.J., 2005) for electrons in water and alanine are presented as a comparison in **Table 1.** The obtained ranges are physically reasonable.

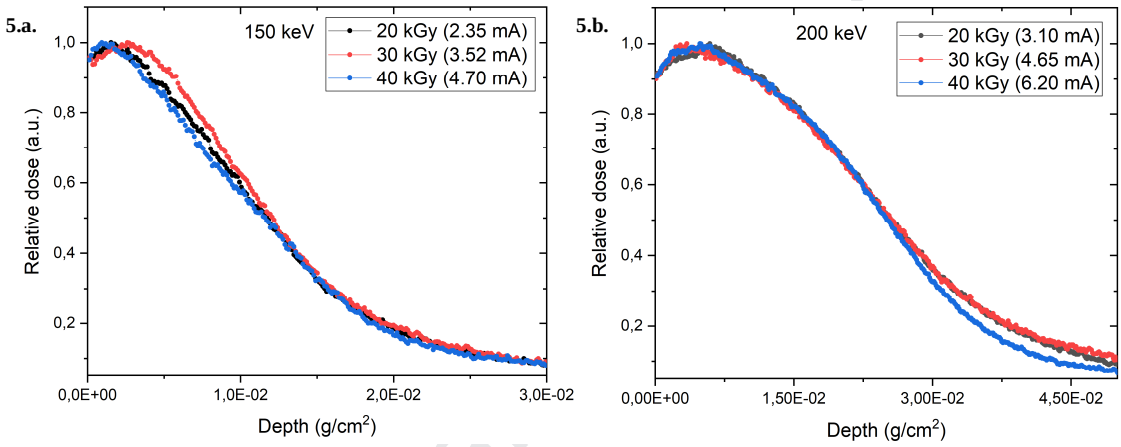

Fig.5. Relative dose-depth profiles of a dosimeter irradiated with **5.a.** 150 keV and **5.b.** 200 keV electron beam

Tab.1. CSDA ranges for electrons in different materials *(Berger M.J., 2005)*

Material	Density at 25□C (g/cm³)	Electron ranges	
		Energy (keV)	CSDA range (g/cm²)
water (liquid)	0.997	150	2.82E-02
		200	4.49E-02
		Energy (keV)	**CSDA range (g/cm²)**
dosimeter	1.163	150	2.87E-02
		200	4.57E-02
		Energy (keV)	**CSDA range (g/cm²)**
alanine	1.420	150	2.89E-02
		200	4.60E-02

Placing the leuco dye in a rigid polymer matrix prevents rotation of the phenyl groups and promotes fluorescence, which signal is strong enough to be used and detected with microscopy resolution. Nevertheless, some improvements to reduce the noise in the readout process, not only digitally, would be pivotal. Some attempts to reduce the amount of scattered light, with placing polarizers (*LPVISC100, ThorLabs*) in the incoming and outcoming light paths, were performed. The approach turned out to be effective; however, the fluorescence signal intensity became essentially lower and difficult to read.

To equalize the uniformity of excitation light, a squared engineered diffuser (*ED1-S50-MD, ThorLabs*) was placed in the illumination plane. It shapes the incident light and as a result, helps to achieve uniform light distribution. Furthermore, the quality of the production process of the dosimeter may also affect the dosimeter response. Thickness reduction of the sample caused better fluorescence response, by reducing the signal coming from deeper layers illuminated simultaneously outside of the focused area, which also reduced the image contrast. However, in order to keep the thickness of the dosimeter sample and achieve better image resolution at the same time, it is planned to perform more precise microscopy techniques readouts, e.g. using light-sheet fluorescence microscopy or two-photon

excitation microscopy.

4. Conclusions

The solid-state, polymer dosimeter that responds to irradiation by the change in its fluorescence intensity response, has been studied. It permits us to measure the relative depth-dose profiles using epi-fluorescence microscope and could be used to verify the efficacy of irradiation procedures for low-energy electron beams. Decreasing the fluorescence background had been performed digitally; however, the manual approach had been also carried out. The obtained relative depth-dose profiles show that the concept of relating the absorbed dose to fluorescence intensities measured by the microscope can be potentially widened to other microscopy techniques. Hence, future studies will focus on using more sensitive light-sheet fluorescence microscopy or two-photon microscopy and performing advanced image processing methods.

5. Acknowledgements

C.E. Andersen for taking professional pictures of the samples.

6. Bibliography

Berejka A.J., C. M. (2014). The evolution of and challenges for industrial raidation processing . *Radiation Physics and Chemistry 94* , 141-146.

Berger M.J., C. J. (2005). *ESTAR, PSTAR, and ASTAR: Computer Programs for Calculating Stopping-Power and Range Tables for Electrons, Protons, and Helium Ions (version 1.2.4)*. (G. M. National Institute of Standards and Technology, Editor) Retrieved from http://physics.nist.gov/Star [18.03.2020].

Bernal-Zamorano M.R., S. N. (2017). Radiochromic and radiofluorogenic 3D solid polymer dosimeter; initial results for high doses. *Journal of Physics: Conference Series, 847*.

Bernal-Zamorano, M., Sanders, N., Lindvold, L., & Andersen, C. (2017). Radiochromic and radiofluorogenic 3D solid polymer dosimeter; effect of the photoinitiator. *Radiation Measurements*, 192-195.

Chiu Y., B. E.-L. (2012). A Study of the Intrinsic Autofluorescence of Poly (ethylene glycol)-co-(L -Lactic acid) Diacrylate. *J Fluoresc 22*, 907-913.

Guozhong Wu, M. W. (2019). *Radiation Technology for Advanced Materials. Chapter One - Radiation Sources and Radiation Processing.* Elsevier Inc.

Helt-Hansen J., M. A. (2010). D-mu- A new concept in industrial low-energy electron dosimetry. *Radiation Physics and Chemistry 79*, 66-74.

IAEA. (2004). Emerging applications of radiation processing. Proceedings of a technical meeting held in Vienna, 28-30 April 2003.

IAEA. (2008). *Trends in radiation sterilization of health care products.* Vienna.

ICRU. (2008). *ICRU Report 80: Dosimetry Systems for Use in Radiation Processing.* Oxford University Press.

McLaughlin W.L., M. A. (1977). Radiochromic plastic films for accurate measurement of radiation absorbed dose and dose distributions. *Radiation Physics Chemistry 10 (2)*, 119-127.